JOURNAL OF PROPULSION AND POWER
Vol. 23, No. 3, May–June 2007

Autoignition Correlations for Pipeline Natural Gas at Low and Intermediate Temperatures

Junhua Chen,* Vincent McDonell,† and Scott Samuelsen‡
University of California, Irvine, California 92697-3550

DOI: 10.2514/1.22184

Advanced combustion devices relying upon premixing of fuel and air to achieve lower emissions are susceptible to issues when presented with fuel variability. A change in the mixture ignition delay time is of particular interest because it will impact the general design requirements for premixing devices. Simple correlations for predicting ignition delay of gaseous fuels are attractive because they can be applied rapidly to design processes. However, the majority of these cannot address gas mixtures as found in practical fuels. As a result, a comprehensive numerical study was performed to determine ignition delay times for natural gas fuels (mixtures of C_{1-3} gases) at low to intermediate temperatures using existing detailed chemical kinetics. To develop correlations that can be rapidly applied, statistical models were employed to encompass fuel compositions and operating conditions. The resulting regression expression for ignition delay as a function of composition is compared with existing global expressions for ignition delay found in the literature. Temperatures from 773 to 1573 K and pressures from 1 to 15 atm were evaluated at equivalence ratios from 0.4 to 1.0. The fuels considered include different mixtures of methane (80–100% volume), ethane (0–20% volume), and propane (0–20% volume). Analyses were performed to evaluate the correlations and the detailed chemical kinetics mechanisms. Recommendations are provided regarding which expression to use under which circumstances.

I. Introduction

ADVANCED combustion devices incorporate premixing of the fuel and air to reduce peak combustion temperatures and thereby reduce NOx emissions [1]. At the same time, increased averaged temperatures and pressure ratios are desired to increase the thermodynamic efficiency. The need to premix while increasing combustor inlet temperatures and pressures leads to a required understanding of the conditions under which autoignition will occur. Further, in light of fuel variability currently found in natural gas [2] and liquefied natural gas (LNG), which is expected to play an increasing role in the future, knowledge of how variation in pipeline fuel composition impacts autoignition is also required.

To address these requirements, different analytical approaches can be taken that are based on models of varying levels of sophistication. At the heart of the model is a reaction mechanism that describes the time-varying behavior of the fuel/oxidizer mixture as a function of temperature, pressure, and mixture composition. Chemical reaction mechanisms can be comprehensive, reduced, or global, with declining numbers of reactions and species.

For screening or quick analysis, global mechanisms are of high engineering value. As a result, simplified (i.e., global) expressions for ignition delay time have been developed, as shown in Table 1. It is noted that most of the autoignition correlations associated with natural gas have focused on *pure* methane rather than mixtures of species. Only a handful of studies have examined the effect of fuel composition on the autoignition time of natural gas, and only one of the global expressions shown in Table 1 even attempts to deal with nonmethane compounds and does so by lumping all C_{2+} species as one specie and is limited to high temperatures (greater than 1300 K) [3]. Tan et al. [4] provided experimental and simulation kinetic data for oxidation of natural gas blends ($CH_4/C_2H_6/C_3H_8$), but did not provide a simple autoignition delay time correlation. Because of the inherent complexity of ignition [5], these simplified models may not be able to capture the details required to account for variations in fuel composition for the range of conditions found in advanced combustion systems. Hence, the existing global expressions are not useful in predicting the potential impact of nonmethane hydrocarbons in *practical* pipeline fuels on autoignition for many applications.

To achieve more precise simulations of autoignition, albeit with much greater complexity and time requirements, a comprehensive reaction mechanism with all possible elementary reactions and different reaction schemes observed in physical experiments is desired. Although the comprehensive mechanisms should be expected to provide more accurate results and capture fuel composition effects, using them requires specialized software to solve a large set of simultaneous equations and considerable user expertise in the operation of the code and/or the interpretation of the results produced.

In summary, no suitable simple design guide is available to explore the extent to which fuel composition impacts ignition delay for many advanced combustion devices, especially the lower temperatures found in gas turbine applications. Although highly sophisticated detailed chemistry models can be used to attain accurate results, a tool with an intermediate level of sophistication and ease of use is desired.

II. Objective and Approach

The objective of the present study is to develop expressions for ignition delay for gaseous fuels with differing hydrocarbon species over a wide range of temperatures and pressures that can be used for quick screening assessments using a spreadsheet or simply coded analysis program. The principle focus is on the low and intermediate temperature regions.

The approach taken is to use a number of comprehensive hydrocarbon combustion mechanisms to develop regression-based correlations. The correlations developed are evaluated through comparisons with existing global expressions. To support recommendations for which correlations to apply for a given

Received 2 January 2006; revision received 5 February 2006; accepted for publication 17 July 2006.

*Graduate Student Researcher, currently GE Energy, 1831 East Carnegie Avenue, Santa Ana, CA 92705. Member AIAA.

†Associate Director, UCI Combustion Laboratory, 323 East Peltason Drive, Room 221. Senior Member AIAA.

‡Director, UCI Combustion Laboratory, Professor of Mechanical, Aerospace, and Environmental Engineering, 323 East Peltason Drive, Room 221. Senior Member AIAA.

Table 1 Literature autoignition correlations for methane and natural gas

Investigation	Correlation	Conditions
[3]	$t = 1.77 \times 10^{-14} \exp(18,693/T)[O_2]^{-1.05}[CH_4]^{0.66}[HC]^{-0.39}$	$T = 1300$–2000 K, $P = 3$–15 atm, $\phi = 0.45$–1.25
[14]	$t = 1.26 \times 10^{-14}[CH_4]^{-0.02}[O_2]^{-1.20} \exp\left(\frac{32,700}{RT}\right)$	$T > 1300$ K, CH_4, lower pressure, fuel lean and rich
[14]	$t = 4.99 \times 10^{-14}[CH_4]^{-0.38}[O_2]^{-1.31} \exp\left(\frac{19,000}{RT}\right)$	$T < 1300$ K, CH_4, higher pressure, fuel rich
[15]	$t = 2.21 \times 10^{-14} \exp(22,659/T)[O_2]^{-1.05}[CH_4]^{0.33}$	$T = 1250$–2500 K, CH_4
[16]	$t = 2.77 \times 10^{-12} \exp\left(\frac{20,012}{RT}\right)[O_2]^{-1.0}$	CH_4
[17]	$t = \frac{2.60 \times 10^{-15}[O_2]_0^{-4/3}[CH_4]_0^{1/3}}{T_0^{-0.92} \exp(-13,180/T_0)}$	$T < 1300$ K, CH_4
[17]	$t = 6.25 \times 10^{-16}[CH_4]_0^{1/3}[O_2]^{-4/3} \exp\left(\frac{23,000}{RT_0}\right)$	$T > 1300$ K, CH_4
[18]	$t = A \exp\left(\frac{52.9 \text{ kcal/mol}}{RT}\right)[CH_4]^{-1.0}[O_2]^{-1.0}$	Fuel rich, CH_4
[19]	$t \propto \frac{1}{A} \exp\left(\frac{25 \text{ kcal/kg-mol}}{R_u T}\right)[O_2]^{-0.80}[CH_4]^{-0.19} P^{-0.99} T^{-0.5}$	$T = 727$–650°C, $P = 7$–10 atm, CH_4
[20]	$t = 4.05 \times 10^{-15}[CH_4]^{0.33}[O_2]^{-1.05} \exp\left(\frac{51,800}{RT}\right)$	Up to 480 atm

condition, the details of how each of the comprehensive mechanisms captures the role of the higher hydrocarbons are evaluated through sensitivity analysis.

III. Model Development

A. Mechanisms

In the present study, three detailed chemical reaction mechanisms were used: Ribaucour or C5 [6], Konnov [7], and GRI-Mech Version 3.0. [8]. These mechanisms have differing numbers of species and elementary reactions. The C5 mechanism was developed for pentane and therefore should also capture the key behaviors of smaller molecules. It features 418 species and 1956 elementary reactions. Of particular note is that this mechanism was validated at low temperatures (640–900 K), which makes it of particular interest for gas turbine applications. The Konnov mechanism features 127 species and 1200 reactions and validation against a number of shock tube studies. Of the three, GRI-Mech Version 3.0 is generally the most well-known. It features 53 species and 325 elementary reactions and is intended to be applied to natural gas combustion. Version 3.0 has purposefully added some propane chemistry to address the higher hydrocarbons that might be found in pipeline gas. The code has been validated over a temperature range from 1000 to 2500 K.

A constant-pressure, homogeneous closed system is assumed and all parameters are a function only of time. Autoignition delay times are obtained at different initial conditions (temperature, pressure, and equivalence ratio) and fuel compositions. The Aurora® module within CHEMKIN Version 3.7 [9] is used to solve the problem to provide temperature and species evolution history as a function of time.

B. Ignition Definitions

An additional complexity for a study of this type is that no standard definition of ignition exists [10,11]. Hence, data are presented in different ways and the choice of coefficients in the correlations becomes challenging. As a result, further evaluation of the agreement among existing studies is needed. For example, most experimental studies have used shock tube techniques, which focus on higher-temperature regions (1000 to 2500 K), whereas continuous flow reactors or rapid compression machines can typically achieve relatively low temperature (generally less than 1000 K). Furthermore, although several validated detailed chemical kinetics mechanisms exist for natural gas fuels, no systematic modeling work has been undertaken to develop autoignition correlations for low to intermediate-temperature ranges.

Experimentally, the onset of ignition is usually inferred from 1) an abrupt rise in pressure or temperature, 2) a large spike in light emission, or 3) the time history of an intermediate species such as OH or CH^* (excited CH radicals, for which the concentration can be inferred from $C_2H + O \rightarrow CH^* + CO$ [12]). For combustion, rapid energy release, indicated by the rapid rise in temperature, is perhaps the most meaningful indicator. As a result, in the present study, the maximum rate of temperature increase has been used to define ignition.

To efficiently develop an expression for ignition delay as a function of fuel composition, a statistically designed matrix consisting of 70 simulations was developed for the factors shown in Table 2. Investigations were carried out for both low- (773–1000 K) and intermediate-temperature (1000–1573 K) ranges. The ignition properties in the present case were studied with three fuel components: methane, ethane, and propane. Although other hydrocarbons may be found in typical pipeline mixtures, these three species capture a wide range of the expected behavior. It has been noted that methane and ethane represent extremes of reactivity, although larger ($C_{>2}$) alkane hydrocarbons have intermediate ignition properties due to their mixed production of H and CH_3 [13]. Hence, in principle, these three species reflect the extremes in reactivity, along with an intermediately reactive species.

Conducting an analysis of variance (ANOVA) on the calculated results produces analytical expressions for the response (autoignition delay times) as a function of the controlled parameters (in this case, fuel composition, temperature, pressure, and equivalence ratio) in the design space (ranges of controlled parameters). Because the design crosses a mixture with other factors, the results produced are often referred to as crossed models (CMs). The CMs developed are

Table 2 Fuel composition and operational parameters for crossed design

	Unit	Min	Max
Response			
Ignition delay time	Sec	NA	NA
Fuel composition			
Composition A, CH_4	% vol	80	100
Composition B, C_2H_6	% vol	0	20
Composition C, C_3H_8	% vol	0	20
Operating parameter			
Factor D, pressure	atm	1	15
Factor E, temperature[a]	K	773	1000
Factor F, equiv ratio	None	0.4	1
Geometric parameter			
None	NA	NA	NA

[a]For intermediate-temperature range, $T = 1000$ to 1573 K.

classified by temperature range and the detailed chemistry mechanism used. The models developed in the current study include the following:

1) CM 1 is a low-temperature C5 mechanism.
2) CM 2 is a low-temperature Konnov mechanism.
3) CM 3 is an intermediate-temperature C5 mechanism.
4) CM 4 is an intermediate-temperature Konnov mechanism.
5) CM 5 is an intermediate-temperature GRI-Mech Version 3.0 mechanism.

The resulting correlations from these models appear in the form shown in Eq. (1).

$$\begin{aligned}\log_{10}\tau_{\text{ign}} &= \alpha_1 X_{\text{CH}_4} + \alpha_2 X_{\text{C}_2\text{H}_6} + \alpha_3 X_{\text{C}_3\text{H}_8} + \alpha_4 X_{\text{CH}_4} P + \alpha_5 X_{\text{CH}_4} T \\ &+ \alpha_6 X_{\text{CH}_4}\phi + \alpha_7 X_{\text{C}_2\text{H}_6} P + \alpha_8 X_{\text{C}_2\text{H}_6} T + \alpha_9 X_{\text{C}_2\text{H}_6}\phi + \alpha_{10} X_{\text{C}_3\text{H}_8} P \\ &+ \alpha_{11} X_{\text{C}_3\text{H}_8} T + \alpha_{12} X_{\text{C}_3\text{H}_8}\phi + \alpha_{13} X_{CH_4} P^2 + \alpha_{14} X_{\text{CH}_4} T^2 \\ &+ \alpha_{15} X_{\text{CH4}}\phi^2 + \alpha_{16} X_{C_2H_6} P^2 + \alpha_{17} X_{C_2H_6} T^2 + \alpha_{18} X_{C_2H_6}\phi^2 \\ &+ \alpha_{19} X_{\text{C}_3\text{H}_8} P^2 + \alpha_{20} X_{\text{C}_3\text{H}_8} T^2 + \alpha_{21} X_{\text{C}_3\text{H}_8}\phi^2 + \alpha_{22} X_{\text{CH}_4} PT \\ &+ \alpha_{23} X_{\text{CH}_4} P\phi + \alpha_{24} X_{\text{CH}_4} T\phi + \alpha_{25} X_{\text{C}_2\text{H}_6} PT + \alpha_{26} X_{\text{C}_2\text{H}_6} P\phi \\ &+ \alpha_{27} X_{\text{C}_2\text{H}_6} T\phi + \alpha_{28} X_{\text{C}_3\text{H}_8} PT + \alpha_{29} X_{\text{C}_3\text{H}_8} P\phi + \alpha_{30} X_{\text{C}_3\text{H}_8} T\phi \end{aligned} \quad (1)$$

where X_{CH_4} is the volumetric fraction of CH_4 in natural gas (0.80–1.00); $X_{\text{C}_2\text{H}_6}$ is the volumetric fraction of C_2H_6 in natural gas (0.00–0.20); $X_{\text{C}_3\text{H}_8}$ is the volumetric fraction of C_3H_8 or larger hydrocarbons in natural gas (0.00–0.20); P is the pressure, atm; T is the temperature, K; ϕ is the equivalence ratio; and $\alpha_1, \cdots, \alpha_{30}$ are the effect coefficients.

The coefficients for each model are summarized in Table 3. The differences between the regression-based ignition delay and the ignition delay based on the full kinetic simulation ranged from 2.16–7.98%. In other words, the correlation shown in Eq. (1) is able to determine ignition delay to within 8% of that determined using the rigorous kinetic calculation using the comprehensive mechanisms.

IV. Model Performance

The models developed were compared against existing ignition delay expressions for pure methane and gas mixtures. In the following section, the reference to the models is CMX, where X refers to the number in Table 3.

A. Pure Methane

As shown in Eq. (2), for pure methane, the correlation reduces to an expression with only 10 terms.

$$\begin{aligned}\log_{10}\tau_{\text{ign}} &= \alpha_1 X_{\text{CH}_4} + \alpha_4 X_{\text{CH}_4} P + \alpha_5 X_{\text{CH}_4} T + \alpha_6 X_{\text{CH}_4}\phi \\ &+ \alpha_{13} X_{\text{CH}_4} P^2 + \alpha_{14} X_{\text{CH}_4} T^2 + \alpha_{15} X_{\text{CH4}}\phi^2 + \alpha_{22} X_{\text{CH}_4} PT \\ &+ \alpha_{23} X_{\text{CH}_4} P\phi + \alpha_{24} X_{\text{CH}_4} T\phi \end{aligned} \quad (2)$$

To compare the results from Eq. (2) with existing expressions, calculated ignition delay times for the following conditions were computed:

1) The oxidant was air (21% oxygen and 79% nitrogen).
2) The equivalence ratio was 1.0.
3) The pressure was $P = 1.0$ and 15.0 atmospheres.
4) The temperature was 773–1573 K.

Figures 1 and 2 present results at 1 atmosphere and 15 atmospheres, respectively. Because the expression from Spadaccini and Colket cannot be applied to concentrations of nonmethane hydrocarbons of zero, 0.0001% was assigned to the [HC] term to facilitate comparison. Because the majority of the global expressions shown in Table 1 were developed for pure methane, it might be expected that all of the correlations should provide consistent results. At 1 atm (Fig. 1), discrepancies (up to three orders of magnitude) are found among the global expressions. The results in the intermediate-temperature range of $1000 < T < 2000$ K are bounded between upper values (Spadaccini and Colket [3] and Petersen et al. [14]) and minimum values (Krishman and Ravikumar [15], Walker et al. [16], and CM 4). Two existing correlations (Krishman and Ravikumar [15] and Li and Williams [17]) and CM 3 and CM 5 exhibit consistent behavior in the intermediate-temperature range.

Table 3 Coefficients for Eq. (1) for each model

	CM 1	CM 2	CM 3	CM 4	CM 5
α_1	2.071E + 01	2.357E + 01	8.782E + 00	8.113E + 00	1.246E + 01
α_2	2.868E + 01	3.215E + 01	2.555E + 01	1.994E + 01	2.416E + 00
α_3	−4.231E + 01	1.973E + 01	−1.443E − 01	3.383E + 00	1.027E + 01
α_4	−1.384E − 01	−1.132E − 01	−1.771E − 01	−1.064E − 01	−1.933E − 01
α_5	−3.568E − 02	−4.177E − 02	−1.095E − 02	−1.150E − 02	−1.680E − 02
α_6	−2.238E + 00	−1.947E + 00	−6.264E − 01	−1.116E + 00	−7.061E − 03
α_7	−2.662E − 01	−1.735E − 01	−1.804E − 01	−1.469E − 01	7.551E − 01
α_8	−4.909E − 02	−5.673E − 02	−4.171E − 02	−3.201E − 02	−1.515E − 02
α_9	1.297E + 00	1.219E + 00	1.156E + 00	1.766E + 00	−1.040E + 00
α_{10}	−1.183E + 00	−8.154E − 02	−3.921E − 01	−3.691E − 02	−3.201E − 01
α_{11}	1.075E − 01	−2.779E − 02	3.115E − 04	−9.929E − 03	−1.393E − 02
α_{12}	3.369E + 00	−1.484E + 00	3.984E + 00	3.746E + 00	7.354E + 00
α_{13}	6.335E − 03	4.519E − 03	4.097E − 03	4.051E − 03	4.583E − 03
α_{14}	1.518E − 05	1.760E − 05	2.076E − 06	2.616E − 06	4.306E − 06
α_{15}	5.485E − 01	6.126E − 01	−2.772E − 01	8.077E − 02	3.781E − 02
α_{16}	1.379E − 04	1.787E − 03	1.418E − 02	8.333E − 03	−2.055E − 03
α_{17}	1.871E − 05	2.283E − 05	1.273E − 05	9.073E − 06	5.996E − 06
α_{18}	1.516E + 00	1.637E − 01	−1.679E + 00	−1.679E + 00	4.271E + 00
α_{19}	1.379E − 02	−1.161E − 03	8.739E − 03	6.090E − 03	8.071E − 03
α_{20}	−7.004E − 05	2.967E − 06	−4.479E − 06	1.470E − 06	1.373E − 06
α_{21}	−4.783E + 00	−1.515E + 00	−2.271E + 00	3.918E − 01	−3.423E + 00
α_{22}	−3.912E − 05	−1.454E − 05	3.241E − 05	−1.698E − 05	3.444E − 05
α_{23}	−2.231E − 02	−1.227E − 02	4.842E − 05	8.037E − 03	4.369E − 03
α_{24}	1.569E − 03	1.085E − 03	7.599E − 04	6.889E − 04	1.120E − 05
α_{25}	2.814E − 04	1.461E − 04	−7.649E − 07	4.012E − 05	−3.532E − 04
α_{26}	1.110E − 02	1.073E − 03	−9.066E − 02	−9.446E − 02	−2.781E − 01
α_{27}	−4.607E − 03	−2.535E − 03	1.755E − 03	1.152E − 03	−1.952E − 03
α_{28}	9.089E − 04	9.425E − 05	2.311E − 04	3.243E − 05	1.247E − 04
α_{29}	−2.290E − 02	−1.150E − 02	−1.362E − 01	−1.935E − 01	−2.706E − 02
α_{30}	3.116E − 03	4.124E − 03	7.276E − 04	−1.552E − 03	−1.862E − 03

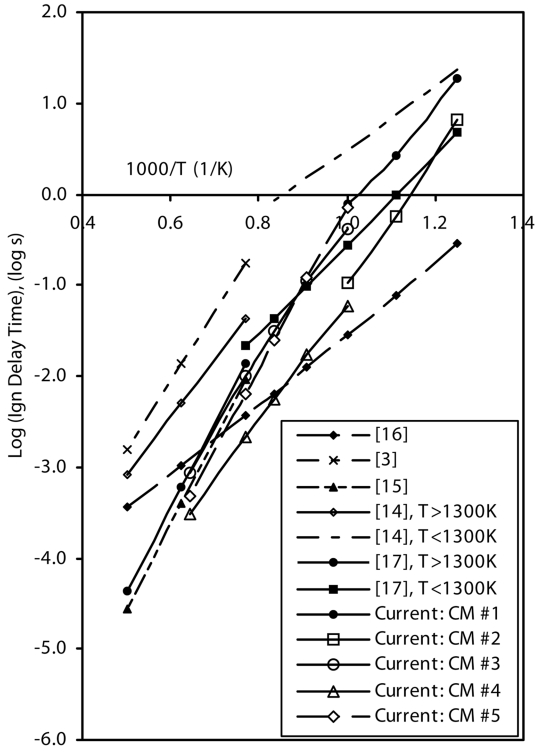

Fig. 1 Comparison of current study with literature correlations for methane autoignition delay time prediction ($P = 1$ atm, $\phi = 1.0$, pure CH_4).

In the lower-temperature range ($T < 1000$ K) for 1 atm, fewer correlations are available. Existing correlations set the upper (Peterson et al. [14]) and the lower (Walker et al. [16]) boundaries, which vary by a factor of 100. The results for the two crossed models developed for the lower-temperature region, CM 1 and CM 2, fall between these two limits, as does the correlation by Li and Williams

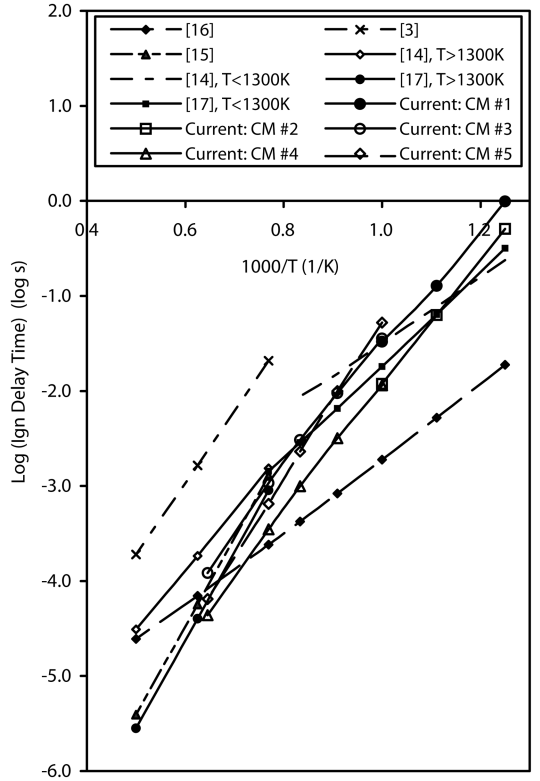

Fig. 2 Comparison of current study to literature correlations for methane autoignition delay time prediction ($P = 15$ atm, $\phi = 1.0$, pure CH_4).

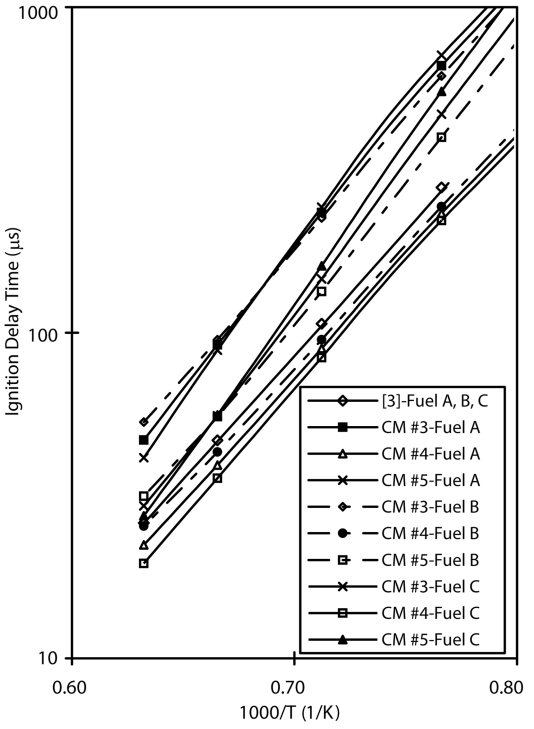

Fig. 3 Model performance compared to Spadaccini and Colket for fuels A, B, and C.

[17]. Interestingly, CM 1 and 2 vary by nearly a factor of 10. Recall that CM 1 explicitly indicates applicability at low temperatures.

At 15 atm (Fig. 2), the overall ignition delay times for pure methane are reduced by an order of magnitude, compared with values at 1 atm. Also, better agreement is found among the existing global correlations and the crossed models developed in the present study. Order-of-magnitude differences are still observed in the intermediate-temperature region ($T > 1000$ K) for the Spadaccini and Colket correlation [3].

In the low-temperature range ($T < 1000$ K) at 15 atm, one correlation [16] falls away from the rest of the results, but the rest of the results vary by less than 50%. Without these two extreme cases [3,16], the results for all five CMs developed in the present study produce results are consistent within themselves and with existing global expressions [14,15,17].

It is pointed out that although CM 2 and CM 4 were both derived from the Konnov mechanism [7], discontinuity is observed at the dividing temperature ($T = 1000$ K) of the two models. This is due to that fact that the two models were correlated separately in different temperature ranges to achieve better fit, which results in discontinuity at $T = 1000$ K.

The comparison of the results for the existing correlations and the models developed in the present study indicates that for pure methane, either CM 3 or CM 5 are recommended for intermediate temperatures ($T > 1000$ K), whereas CM 1 is recommended for 773 K $< T <$ 1000 K. CM 1 is based on a more comprehensive set of reactions. The results also suggest that some of the existing global expressions also provide consistent results with those produced with comprehensive mechanisms. Again, this should be expected for pure methane, because the global expressions were developed for methane.

B. C1–C3 Gas Mixtures

1. Correlation Comparison

For mixtures of species, only one correlation is available [3]. In this correlation, the effects of higher hydrocarbons are combined into a single factor (i.e., the $[HC]$ term in the expression), as shown in Table 1. The underlying assumption is that higher hydrocarbons (C_{2+}) have the same impact on autoignition time. Also, this correlation is valid for relatively high temperatures

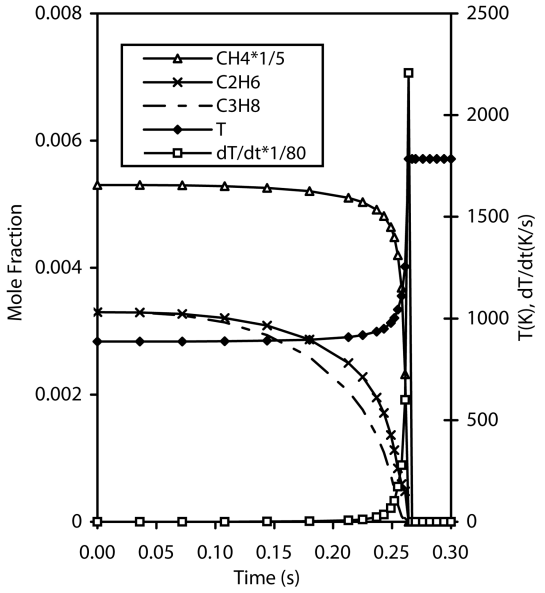

Fig. 4 Fuel concentration evolution for the selected low-temperature case (C5 mechanism [6]; autoignition delay time is 0.261 s).

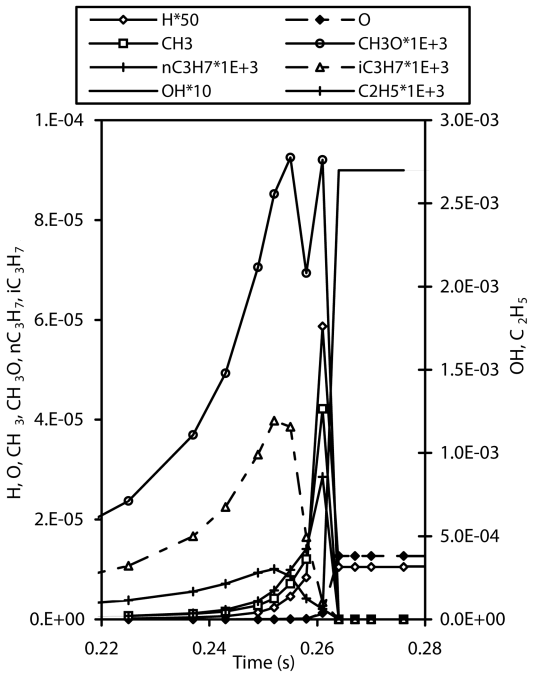

Fig. 5 Concentration (mole fraction) evolution of important intermediates for the selected low-temperature case (C5 mechanism [6]; autoignition time is 0.261 s).

($1300 < T < 2000$ K). As a result, no low-temperature comparison can be conducted (i.e., CMs 1 and 2). Hence, CMs 3, 4, and 5 are compared in the high-temperature range (1300 to 1573 K).

The evaluation was conducted for the following conditions:

1) Fuel A was 90% CH_4, 5% C_2H_6, and 5% C_3H_8.
2) Fuel B was 90% CH_4 and 10% C_2H_6.
3) Fuel C was 90% CH_4 and 10% C_3H_8.
4) The equivalence ratio was 1.0.
5) The pressure was 10 atmospheres.

Figure 3 shows the comparison, and key features include the following:

1) The existing global expression [3] predicts the same ignition delay time for all three fuels, because any higher hydrocarbon is considered to have the same effects on autoignition.

2) The crossed models, based on the three comprehensive mechanisms, indicate sensitivity to specific fuel type, suggesting that different fuel species have different effects on autoignition delay time and cannot be combined into one single term in the expression.

3) In the 1300 to 1600 K range, autoignition times are ranked CM 3 > CM 5 > [3] > CM 4 for a given fuel. The total range varies by 50%.

4) For CM 3, autoignition delay time profiles of the three fuels have different slopes, which indicate different activation energy for different fuel. Also, the lines cross each other at $T \sim 1450$ K (critical temperature, T_c). Fuel C (90% CH_4 and 10% C_3H_8) has a shorter autoignition delay time than fuel B (90% CH_4 and 10% C_2H_6) when $T > T_c$. On the other hand, when $T > T_c$, fuel C has longer autoignition delay time. This is due to the interaction of temperature and fuel composition. Similar interaction of temperature and fuel species is also predicted by CM 5, but at a critical temperature T_c of ~1500 K. CM 4 does not predict temperature-hydrocarbon interaction in the temperature range studied.

For gas mixtures, the models perform similarly from a qualitative point of view, however, differences are observed. The differences stem directly from the chemical kinetic mechanisms, which include the size of species set, completeness of reaction channels, and values of rate coefficients of elementary reactions. To explore this further, additional analyses were conducted.

2. *Role of Ethane and Propane Species*

Species evolution and mechanism comparison were examined using two [6,7] of the detailed mechanisms in the low-temperature range and all three [6–8] mechanisms at intermediate temperature. Recall that the low-temperature limit for GRI-Mech Version 3.0 [8] precludes its inclusion in the low-temperature analysis. The conditions selected for the analysis were as follows:

1) CH_4 in NG was 80% by volume.
2) C_2H_6 in NG was 10% by volume.
3) C_3H_8 in NG was 10% by volume.
4) The oxidant was air (21%O_2 and 79%N_2).
5) The equivalence ratio was 0.4.
6) The mixture pressure was 8 atm.
7) The mixture temperature was 886.5 K (for low temperature) or 1286.5 K (for intermediate temperature).

Figures 4 and 5 present the evolution of species and temperature of the selected low-temperature condition for the C5 mechanism [6]. Figure 4 shows the evolution of fuel species (CH_4, C_2H_6, and C_3H_8), as well as temperature and the rate of change of temperature. Once the combustible mixture is created at $t = 0$, the initiation reactions of the three fuel species occurs and the accumulation of active intermediates and radicals begins immediately, as shown in Fig. 5. During the initiation period, the reactions are relatively slow and the temperature change is small. Eventually, the pool of active intermediates and reactive radicals such as CH_3, H, O, OH, CH_3O,

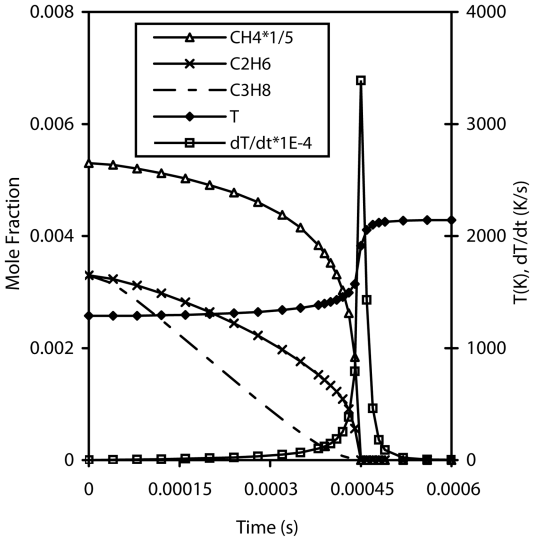

Fig. 6 Evolution of fuel concentration for the selected intermediate-temperature case (C5 mechanism [6]; autoignition time is 4.45×10^{-4} s).

C_2H_5, n-C_3H_7, and i-C_3H_7 (Fig. 5) accumulate sufficiently and initiation reactions rapidly accelerate and lead to autoignition. Most intermediates and radicals are consumed rapidly. Some, such as O and OH, remain until hydrocarbon species are consumed, at which point their concentrations level off at values characteristic of CO oxidation, which is inhibited before autoignition.

During the preignition phase, initiation reactions and fuel consumption overlap. Although small, differences are noted between the consumption rates of the three fuel species. As shown in Fig. 4, fuel consumption occurs throughout the induction period, but methane consumption is slower than either ethane or propane in the early stage. Thus, the two higher hydrocarbons (C_2H_6 and C_3H_8) play important roles in initiating the overall reaction. The mechanism examined here [6] predicts that at 50% of the induction time, less than 0.57% of CH_4 is consumed, whereas 4.55% of C_2H_6 and 7.58% of C_3H_8 are converted to intermediate species. At 90% of the induction time, 93.40% of methane remains, whereas 62.12% of ethane remains unreacted and 45% of the propane remains.

The same case was analyzed using the Konnov mechanism [7], and the autoignition delay time, evolution of the fuel species, and intermediate species were found to be very similar to those shown for the C5 mechanism [6] and are therefore not presented here. A key result for results obtained using both mechanisms is that higher hydrocarbons (ethane and propane) play an important role in promoting reactivity of the mixtures. In addition, both mechanisms suggest that propane (0–20% volume additive to natural gas mixture) is much more reactive in promoting the overall reaction rate at low temperatures.

Results using the C5 mechanism [6] for the intermediate-temperature range are presented in Fig. 6 for $T = 1286.5$ K, whereas all other parameters were kept the same as for the previous low-temperature case. As expected, fuel consumption is much faster than at low temperatures (Fig. 4). Again, propane is consumed more quickly than ethane and methane. Fast initiation reactions of all three hydrocarbon species occur immediately after the creation of the mixture and quickly generate radicals. The concentration profiles of the active radicals and intermediates are presented in Fig. 7. At intermediate temperature, an early and large quantity of active intermediates such as CH_3, C_2H_5, i-C_3H_7, CH_3O, O, H, OH, and n-C_3H_7 are observed. Through the channels of chain-branching and radical propagation reactions, these reactive species exponentially increase the pool of reactively active species and accelerate the overall rate of reaction of the system, which leads to exponentially reduced autoignition delay time or induction time.

The presence of large amounts of C_3H_6, C_2H_5, and i-C_3H_7 and their rapid increase in the early stage of the induction time are related to the rapid thermal decomposition (mainly via $C_3H_8 = CH_3 +$ C_2H_5) or hydrogen abstractions of propane. The production of i-C_3H_7 is more favorable than that of n-C_3H_7. For the higher-temperature example, the temperature sensitivity of the reactivity of propane is again found to be much greater than that of ethane or methane.

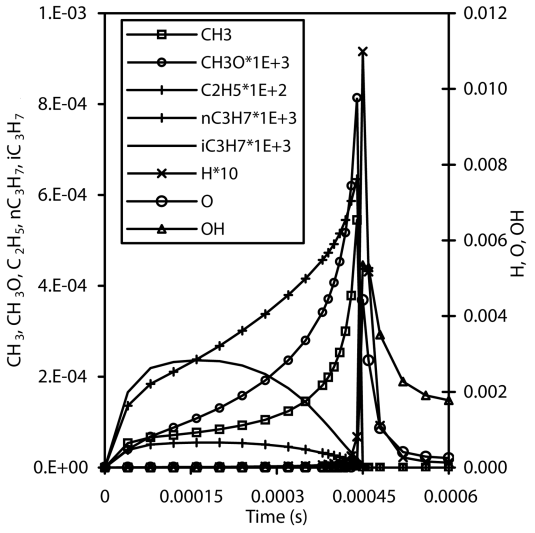

Fig. 7 Concentration (mole fraction) evolution of important intermediates for the selected intermediate-temperature case (C5 mechanism [6]; autoignition delay time is 4.45×10^{-4} s).

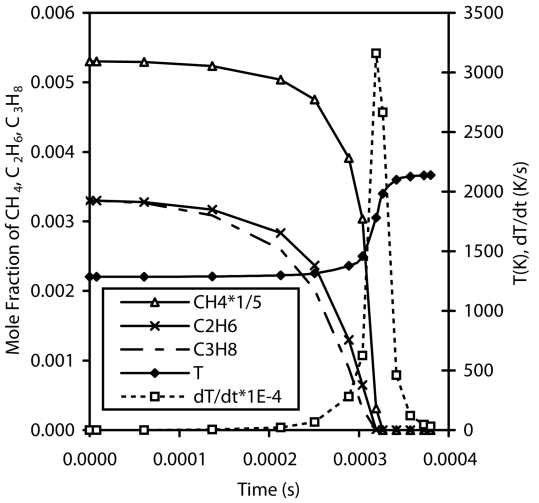

Fig. 8 Fuel concentration evolution for the selected intermediate-temperature case (GRI-Mech Version 3.0 [8]; autoignition delay time is 3.17×10^{-4} s) [8].

Like the results for the low-temperature case, the results produced using the second comprehensive mechanism [7] are qualitatively similar to those found with the first mechanism [6] and are not shown, for brevity. At higher temperature, results for both mechanisms indicate that the different hydrocarbon species have distinct temperature sensitivity. Like the low-temperature findings, propane is found to be the most responsive species to temperature.

At the intermediate-temperature case now considered (1286.5 K), simulations are also possible with the third mechanism [8]. These results are shown in Figs. 8 and 9 and differ from those found with the first two mechanisms [6,7]. The results with GRI-Mech Version 3.0 [8] at intermediate temperatures appear more like those found at low temperature with the first two mechanisms (comparing Fig. 8 to Fig. 4 or Fig. 9 to Fig. 5). The results using the third mechanism do not predict rapid consumption of either ethane or propane at the early stage and indicate that they behave like methane. Rapid consumption

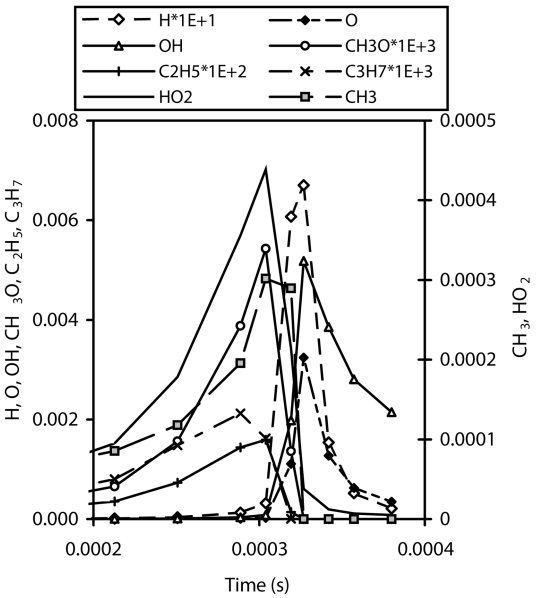

Fig. 9 Concentration (mole fraction) evolution of important intermediate species for the selected intermediate-temperature case (GRI-Mech Version 3.0 [8]; autoignition delay time is 3.17×10^{-4} s).

Table 4 Relative importance of reactions with the greatest positive temperature sensitivity coefficients for intermediate temperature

No.	Reactions	Konnov mech Order	C5 mech Order	GRI-Mech Order
1	$H + O_2 \Leftrightarrow OH + O$	1	1	2
2	$CH_3 + HO_2 \Leftrightarrow CH_3O + OH$	2	2	1
3	$CH_3 + O_2 \Leftrightarrow CH_2O + OH$	3	3	10
4	$C_2H_5(+M) \Leftrightarrow C_2H_4 + H(+M)$	4	×	×
5	$CH_3 + O_2 \Leftrightarrow CH_3O + O$	5	5	5
6	$C_2H_6 + OH \Leftrightarrow C_2H_5 + H_2O$	6	4	3
7	$CH_2O + OH \Leftrightarrow HCO + H_2O$	7	×	9
8	$C_2H_4 + OH \Leftrightarrow C_2H_3 + H_2O$	8	10	6
9	$C_2H_3 + O_2 \Leftrightarrow CH_2HCO + O$	9	7	×
10	$C_3H_8 + OH \Leftrightarrow iC_3H_7 + H_2O$	10	×	×
11	$H + H_2H_4(+M) \Leftrightarrow C_2H_5(+M)$	×	6	×
12	$OH + H_2 \Leftrightarrow H + H_2O$	×	8	×
13	$HCO + M \Leftrightarrow H + CO + M$	×	9	×
14	$CH_3 + C_2H_5(+M) \Leftrightarrow C_3H_8(+M)$	×	×	4
15	$2OH(+M) \Leftrightarrow H_2O_2(+M)$	×	×	7
16	$H + CH_2O(+M) \Leftrightarrow CH_3O(+M)$	×	×	8

Table 5 Relative importance of reactions with the greatest negative temperature sensitivity coefficients for intermediate temperature

No.	Reactions	Konnov mech Order	C5 mech Order	GRI-Mech Order
1	$2CH_3(+M) \Leftrightarrow C_2H_6(+M)$	1	1	1
2	$CH_4 + H \Leftrightarrow CH_3 + H_2$	2	2	4
3	$HO_2 + OH \Leftrightarrow H_2O + O_2$	3	6	6
4	$CH_4 + OH \Leftrightarrow CH_3 + H_2O$	4	3	2
5	$H + O_2(+M) \Leftrightarrow HO_2(+M)$	5	5	×
6	$H + HO_2 \Leftrightarrow H_2 + O_2$	6	×	×
7	$H + HO_2 \Leftrightarrow 2OH$	7	×	×
8	$nC_3H_7 \Leftrightarrow C_2H_4 + CH_3$	8	9	×
9	$CH_3OH(+M) \Leftrightarrow CH_3 + OH(+M)$	9	×	×
10	$C_3H_8 + H \Leftrightarrow nC_3H_7 + H_2$	10	7	5
11	$CH_3 + HO_2 \Leftrightarrow CH_4 + O_2$	×	4	×
12	$CH_3 + H(+M) \Leftrightarrow CH_4(+M)$	×	8	×
13	$CH_2O + H \Leftrightarrow HCO + H_2$	×	10	×
14	$2HO_2 \Leftrightarrow O_2 + H_2O_2$	×	×	3
15	$HO_2 + CH_3 \Leftrightarrow O_2 + CH_4$	×	×	7
16	$CH_3O + O_2 \Leftrightarrow HO_2 + CH_2O$	×	×	8
17	$H + CH_3(+M) \Leftrightarrow CH_4(+M)$	×	×	9
18	$OH + C_3H_8 \Leftrightarrow C_3H_7 + H_2O$	×	×	10

of the three fuel species happens only in the near-ignition regime. As a result, the profiles of important radicals and intermediates are the same as those found in low-temperature conditions. No rapid accumulation of intermediates of propane and ethane such as C_2H_5, C_3H_6, i-C_3H_7 and C_2H_4 is observed in the early stage of the induction period.

GRI-Mech Version 3.0 [8] indicates that ethane is always more important than propane in affecting ignition delay time. In contrast, results generated using the other two mechanisms indicate that the initiation reactions of propane have greater reaction rates than those of ethane, although initiation reactions of both species occur at the early stage of the induction period.

An explanation of the differences observed for the results based on the third mechanism [8] is likely due to the inadequacy of elementary reactions and species for higher hydrocarbons ($C_{>2}$). The third mechanism [8] is relatively small, with 325 reactions among 53 species. The species have only up to three carbons in their structure, and only two C_3 species are included in the mechanism: C_3H_7 and C_3H_8. Considering the hierarchical structure of hydrocarbon reaction mechanism and the possible recombination of fuel intermediates to species with higher carbon content (C_{3+}), GRI-Mech Version 3.0 [8] lacks the ability to simulate mixtures with large amount of C_{3+} species. On the other hand, the C5 mechanism [6] has 1956 elementary reactions among 418 species (up to C_6) and the Konnov mechanism [7] has 1207 elementary reactions among 127 species (up to C_6). The inclusion of more reactions and species enables these two mechanisms to capture the subtleties of the initiation reactions of ethane and propane in the early stage of induction time.

The most significant reactions that promote or inhibit ignition at the time of ignition for the three mechanisms are listed in Tables 4 and 5. The numbers in the columns under each mechanism indicate the importance of the reaction, with 1 indicating the greatest temperature sensitivity and 10 indicating the least sensitivity. X indicates the reaction is not significant, based on the mechanism at the top of the column. The results show that the C5 and Konnov mechanisms have a relatively consistent set of key reactions compared with GRI-Mech Version 3.0.

Most of the reactions with significant positive temperature sensitivity coefficients are chain-branching reactions or reactions that directly or indirectly consume fuel or their intermediates to produce simpler species. The two reactions with the most significant positive temperature sensitivity are

$$H + O_2 = OH + O \qquad CH_3 + HO_2 = CH_3O + OH$$

The CH_3O channel is the most important reaction channel for the conditions studied.

Table 5 shows the reactions with the most significant negative temperature sensitivity coefficients. Again, the C5 and Konnov mechanisms result in a more consistent set of key reactions compared with GRI-Mech. Most are either chain termination reactions or reactions that produce CH_3 and promote reaction inhibition:

$$2CH_3(+M) = C_2H_6(+M)$$

V. Conclusions

A strategy to develop an efficient tool for determining the effect of higher hydrocarbons on ignition delay has been presented. Three detailed chemical kinetic mechanisms were used in the development of the tool. Expressions for ignition delay time as a function of temperature, pressure, equivalence ratio, and fuel composition have been developed for both low- and intermediate-temperature conditions that can be used in a spreadsheet. To determine which model developed is most appropriate for studying the effects of fuel composition, a sensitivity analysis for each mechanism was conducted. Based on the results obtained, it is recommended that CM 3 should be used at intermediate temperatures (1000–1573 K) and CM 1 should be used at low temperatures (773–1000 K). Both of these models were derived using the most comprehensive mechanism considered.

The conclusions from the study are as follows:

1) A model that is simple to implement and can capture the effects of fuel composition, mixture temperature and strength, and pressure is now available for use as a design guide.

2) The presence of higher hydrocarbons in methane reduces ignition delay time significantly and therefore must be considered in any assessment of autoignition. Ethane and propane each impact autoignition characteristics of natural gas fuels in a different manner. An interaction between initial temperature and the role of the particular hydrocarbon species is observed. As a result, depending on the temperature, ethane or propane can be more limiting in determining the ignition delay time.

Acknowledgments

The authors gratefully acknowledge the support from the U.S. Department of Energy and the University Turbine Systems Research program (contract 00-01-SR084CS).

References

[1] Richards, G. A., McMillian, M. M., Gemmen, R. S., Rogers, W. A., and Cully, S. R., "Issues for Low-Emission, Fuel-Flexible Power System," *Progress in Energy and Combustion Science*, Vol. 27, No. 2, 2001, pp. 141–169.

[2] Liss, W. E., Thrasher, W. H., Steinmetz, G. F., Chowdiah, P., and Attari, A., "Variability of Natural Gas Composition in Select Major Metropolitan Areas of the United States," Gas Research Inst., GRI-92/0123, Des Plaines, IL, Mar. 1992.

[3] Spadaccini, L. J., and Colket, M. B., "Ignition Delay Characteristics of Methane Fuels," *Progress in Energy and Combustion Science*, Vol. 20, No. 5, 1994, pp. 431–460.

[4] Tan, Y., Dagaut, P., Cathonnet, M., and Boettner, J.-C., "Oxidation and Ignition of Methane-Propane and Methane-Ethane-Propane Mixtures: Experiments and Modeling," *Combustion Science and Technology*, Vol. 103,1994, pp. 133-151.

[5] Turns, S. R., *An Introduction to Combustion: Concepts and Applications*, 2nd ed., McGraw–Hill, New York, 2000.

[6] Ribaucour, M., Minetti, R., Sochet, L. R., Curran, H. J., Pitz, W. J., and Westbrook, C. K., "Ignition of Isomers of Pentane: An Experimental and Kinetic Modeling Study," *Proceedings of the Combustion Institute*, Vol. 28, Combustion Inst., Pittsburgh, PA, 2000, pp. 1671–1678.

[7] Konnov, A. A., "Development and Validation of a Detailed Reaction Mechanism for the Combustion of Small Hydrocarbons." *Twenty-Eighth International Symposium on Combustion*. Combustion Inst., Pittsburgh, PA, 2000 p. 317.

[8] *GRI-Mech Ver. 3.0* [online database], http://www.me.berkeley.edu/gri_mech/ [retrieved Aug. 2003].

[9] CHEMKIN Collection, Software Package, Ver. 3.7, Reaction Design, Inc., San Diego, CA, 2002.

[10] Akbar, R., Kaneshige, M., Schultz, E., and Shepherd, J., "Detonation in H_2-N_2O-CH_4-NH_3-O_2-N_2 Mixtures," Explosion Dynamics Lab., Graduate Aeronautical Labs., California Inst. of Technology, Rept. FM97-3, Pasadena, CA, 2000.

[11] Hall, J. M., Rickard, M. J. A., and Petersen, E. L., "Comparison of Characteristic Time Diagnostics for Ignition and Oxidation of Fuel/Oxidizer Mixtures Behind Reflected Shock Waves," *Combustion Science and Technology*, Vol. 177, No. 3, 2005, pp. 455–483.

[12] Glassman, I., *Combustion*, 3rd ed., Academic Press, San Diego, CA, 1996.

[13] Westbrook, C. K., "Chemical Kinetics of Hydrocarbons Ignition in Practical Combustion Systems," *Proceedings of the Combustion Institute*, Vol. 28, Combustion Inst., Pittsburgh, PA, 2000, pp. 1563–1577.

[14] Petersen, E. L., Davidson, D. F., and Hanson, R. K., "Ignition Delay Times of Ram Accelerator CH4/O2/Diluent Mixtures," *Journal of Propulsion and Power*, Vol. 15, No. 1, 1999, pp. 82–91.

[15] Krishman, K. S., and Ravikumar, R., *Combustion Science and Technology*, Vol. 24, 1981, p. 239.

[16] Walker, D. W., Diehl, L. H., Strauss, W. A., and Edse, R., "Investigation of the Ignition Properties of Flowing Combustible Gas Mixtures," U.S. Air Force Rept. AFAPL-TR-69-82, 1969.

[17] Li, S. C., and Williams, F. A., "Reaction Mechanism for Methane Ignition," *Journal of Engineering for Gas Turbines and Power*, Vol. 124, No. 3, July 2002, pp. 471–480.

[18] Asaba, T., Yoneda, K., Kakihara, N., and Hikita, T., "A Shock-Tube Study of Ignition of Methane-Oxygen Mixtures," *9th Symposium (International) on Combustion*, Combustion Inst., Pittsburgh, PA, 1963, p. 193.

[19] Lefebvre, A. H., Freeman, W., and Cowell, L., "Spontaneous Ignition Delay Characteristics of Hydrocarbon Fuel/Air Mixtures," NASA CR 175064, 1986.

[20] Petersen, E. L., Rohrig, M., Davidson, D. F., Hanson, R. K., and Bowman, C. T., "High-Pressure Methane Oxidation Behind Reflected Shock Tube Waves," *26th Symposium (International) on Combustion*, Combustion Inst., Pittsburgh, PA, 1996, pp. 799–806.

C. Avedisian
Associate Editor